Available online at www.sciencedirect.com
SCIENCE DIRECT®
Chemical Physics 284 (2002) 233–251
Chemical Physics
www.elsevier.com/locate/chemphys

Stationary states of non-linear oscillators driven by Lévy noise

A. Chechkin[a,b,*], V. Gonchar[a], J. Klafter[c], R. Metzler[d,e], L. Tanatarov[a]

[a] Institute for Theoretical Physics, National Science Center, Kharkov Institute of Physics and Technology, Akademicheskaya St.1, 61108 Kharkov, Ukraine
[b] Erstes Mathematisches Institut, FB Mathematik & Informatik Freie Universitaet Berlin, Arnimalee 3, D-14195 Berlin, Germany
[c] School of Chemistry, Sackler Faculty of Exact Sciences, Tel Aviv University, Ramat Aviv, Tel Aviv 69978, Israel
[d] Department of Physics, Massachusetts Institute of Technology, 77 Massachusetts Ave., Rm 12-109, Cambridge, MA 02139, USA
[e] NORDITA, Blegdamsvej 17, DK-2100 København Ø, Denmark

Received 30 November 2001

Abstract

We study the probability density function in the stationary state of non-linear oscillators which are subject to Lévy stable noise and confined within symmetric potentials of the general form $U(x) \propto x^{2m+2}/(2m+2)$, $m = 0, 1, 2, \ldots$. For $m \geqslant 1$, the probability density functions display a distinct bimodal character and have power-law tails which decay faster than those of the noise probability density. This is in contrast to the Lévy harmonic oscillator $m = 0$. For the particular case of an anharmonic Lévy oscillator with $U(x) = ax^2/2 + bx^4/4$, $a > 0$, we find a turnover from unimodality to bimodality at stationarity.

Keywords: Lévy flights; Fractional derivative; Non-linear oscillator; Fractional kinetic equation; Lévy stable noise

1. Introduction

The classical problem of Brownian motion has been a paradigm whose universality had been unchallenged only until recently [1–6]. Brownian motion describes the motion of small macroscopic particles in a liquid or a gas which experience unbalanced bombardments due to surrounding atoms, and hence reveals the atomistic structure of the medium in which the motion occurs.

There exist two alternative approaches to Brownian motion: (i) the Langevin approach which mimics the influence of the "bath" of surrounding molecules in terms of a mean field-type, time-dependent stochastic force; and (ii) the kinetic approach based on transport equations of the Boltzmann type in which the collisions are considered in terms of the cross-section between the test particle and a given close particle. In what follows, we concentrate on the Langevin approach.

Classically, the force experienced by the test particle is assumed to be composed of a deterministic contribution that stems from an external force and an effective friction force, and a stochastic part which describes fluctuations caused by

* Corresponding author. Tel.: +7-572-35-1183; fax: +7-572-35-1738.
E-mail address: achechkin@kipt.kharkov.ua (A. Chechkin).

0301-0104/02/$ - see front matter
PII: S0301-0104(02)00551-7

the bath. Usually, the stochastic force is assumed to be white Gaussian noise, i.e., (i) the correlation time of the fluctuations is much smaller than the time scale of the macroscopic motion (e.g., the correlation times of the velocities and the positions); and (ii) the interaction with the bath is weak in the sense that each collision leads to a marginal change of the velocity and position of the Brownian particle. Mathematically, the latter statement is strongly connected with the Central Limit Theorem which states that the normalized sum of independent, identically distributed (i.i.d.) random variables with *finite variance* converges to the Gaussian probability distribution [7,8].

In the presence of white Gaussian noise, the stochastic Langevin equation corresponds to a Fokker–Planck Markovian deterministic equation which governs the system equilibration towards the Gibbs–Boltzmann equilibrium and controls the relaxation of the probability density function (PDF) $f(x,v,t)$ in the phase space spanned by the position and velocity coordinates x and v. Its underdamped and overdamped limits, the Rayleigh equation and the Einstein–Smoluchowski equation (ESE), determine the temporal evolution of the velocity PDF $f(v,t)$ and the position PDF $f(x,t)$. The collision integrals in these deterministic equations are local. The deterministic equations contain linear differential operators in velocity and position, respectively.

Over the past two decades it has become obvious that anomalous random processes and related anomalous diffusion phenomena are almost ubiquitous in nature [9–12]. Accordingly, the observed phenomena show clear deviations from ordinary Brownian motion. In particular, the mean squared displacement no longer grows linearly in time; instead, it grows slower (subdiffusion) or faster (superdiffusion), or even diverges. There exist numerous examples of anomalous diffusion in a broad range of fields, cf. the reviews [10,13] and the references therein. It is a basic consequence of such systems that their description should lie beyond the traditional Fokker–Planck–Smoluchowski framework. This is due to the fact that some of the assumptions that lead to classical Brownian motion are violated, and therefore have to be relaxed in order to properly account for such phenomena. In the following, we consider white (δ-correlated) noise whose distribution is Lévy stable, i.e., we consider random processes which are subject to the Generalized Central Limit Theorem. According to the latter, Lévy stable distributions are the limit ones for properly normalized sums of i.i.d. random variables with *diverging variance* [7,14]. Therefore, they are natural generalizations to the Brownian processes.

Lévy stable laws possess power-law tails of the form $\sim |x|^{-\alpha-1}$, where α, the Lévy index, ranges in the interval $0 < \alpha < 2$. This means that moments of order $q \geqslant \alpha$ diverge. From a physical point of view, these Lévy flights are the results of strong collisions between the test particle and the surrounding environment.

Some mathematical aspects of the Lévy driven stochastic differential equations are discussed in [15–18]. While it might be speculated whether the use of Lévy noise within a Langevin-type approach is an adequate way to grasp peculiarities of the time evolution and the stationary states of various systems, it seems clear that the scale-free self-similar nature of Lévy stable distributions gives rise to the occurrence of large increments of the velocity and position coordinates during small time increments, violating the local character of the collision integrals in the traditional deterministic equations. Levy flights can be studied therefore as paradigm systems for going beyond Brownian motion, keeping in mind that for a massive particle, they are only an approximation, since such a particle has a finite maximum velocity and extremely long jumps should experience a time penalty [11,12,19]. However, the Lévy approach is able to reproduce essential features of such systems, and therefore it is justified to pursue such a study.

The non-local character brought about by the Lévy noise leads to the replacement of the local spatial derivatives in the diffusion term of the ESE by a *fractional derivative* [13,20]. The resulting equation is the fractional ESE (FESE), which is a representative of the class of fractional Fokker–Planck equations [13]. Very recently, the fundamental solution of space-time fractional diffusion equation was obtained in terms of Mellin–Barnes integral representation [21]. We also note that relaxation and oscillation type ordinary differential

equations of fractional order were considered in [22].

The role of Levy noise in various systems was investigated earlier [23–26]. A derivation on the grounds of generalized continuous time random walks was presented in [20]. It was shown in [27,28] that the relaxation of an harmonic Lévy oscillator tends towards a stable PDF of the same Lévy index as the Lévy noise, i.e., the stationary PDF has a long tail with slow decay.

In the present paper we consider three types of overdamped *non-linear* oscillators driven by Lévy noise. The three Lévy oscillators are characterized by the following potentials $U(x)$:

Type 1. $U(x) = bx^4/4$ (quartic Lévy oscillator).

Type 2. $U(x) = ax^2/2 + bx^4/4$, $a > 0$ (anharmonic Lévy oscillator).

Type 3. $U(x) = bx^{2m+2}/(2m+2), m = 1,2,\ldots$ (strongly non-linear Lévy oscillator).

Such non-linear oscillators play important roles in the theory of Brownian motion in open auto-oscillation systems [29], in the theory of dynamical chaos [30,31], and they might have various other applications [32].

The main results of the current work are two interesting new properties of the stationary states for non-linear oscillators driven by Lévy noises: (i) bimodality of the PDFs, and (ii) power-law asymptotics, which decay faster than the PDF of the noise, thus providing the finiteness of the variance. The latter suggests that the non-linear nature of the Lévy oscillator leads to the confinement of the noise. We obtain these properties by analytical solutions of the FESE as well as numerical solution of the corresponding Langevin equation. Both properties, the bimodality and the steep power-law asymptotics are, in fact, the manifestation of the Lévy statistics of the noise and of the non-linearity of the force field in the FESE.

The paper is organized as follows. In Section 2 the general formulation is introduced, and the stationary solutions for two particular cases are recalled; namely, the non-linear Brownian oscillator and the harmonic Lévy oscillator. In Sections 3–5 the properties of stationary solutions for the three types of non-linear Lévy oscillators are investigated. In Section 6 the numerical algorithm and the results of numerical modeling based on the Langevin equations are presented. Finally, in Section 7 the main results are summarized.

2. General formulation

Let us start by studying the properties of stationary PDFs of non-linear overdamped oscillators exhibiting Lévy flights. The starting Langevin equation is

$$\frac{\mathrm{d}x}{\mathrm{d}t} = \frac{F(x)}{m\gamma} + Y(t), \tag{2.1}$$

where $F = -\mathrm{d}U/\mathrm{d}x$, U is the potential energy function, m is the particle mass, γ is the friction coefficient, and $Y(t)$ is a stationary white Lévy noise.

Since the Lévy processes are less known than their Gaussian counterpart, the term "white Lévy noise" requires more comments. At first, we note that, from the mathematical viewpoint [33], white Gaussian noise or Lévy noise are stationary sequences of the independent increments of the Wiener (non-stationary Gaussian) or Lévy stable processes, respectively. In physics literature, see, e.g., [1,2], the white Gaussian noise is defined as a stationary random process, such that the integral of it over time is the Wiener process. Similarly, white Lévy noise $Y(t)$ can be defined such that the process

$$L(\Delta t) = \int_t^{t+\Delta t} \mathrm{d}\tau\, Y(\tau), \tag{2.2}$$

which is the time integral over an increment Δt is an α-stable process with stationary independent increments [34]. We restrict ourselves to symmetric probability laws with the characteristic functions

$$\hat{p}_L(k, \Delta t) = \exp(-D|k|^{\alpha}\Delta t), \tag{2.3}$$

where α is the Lévy index, $0 < \alpha \leq 2$, and the positive parameter D has the meaning of a measure of the intensity of the Lévy noise in the Langevin equation. In the theory of stable probability laws, $D^{1/\alpha}$ is called the scale parameter [33].

If $\alpha = 2$, Eq. (2.3) is a characteristic function of the Wiener (Gaussian) process, and the kinetic equation for the PDF $f(x,t)$ is the ESE leading to the Boltzmann stationary distribution. Instead, the non-Gaussian Lévy statistics of the noise in the

Langevin equation provides us with a simple and straightforward (at least, from a methodical point of view) possibility to consider non-Boltzmann stationary states. Thus, if $\alpha < 2$, then by applying the procedure described in [27], we arrive at the FESE in an external force field:

$$\frac{\partial f}{\partial t} = -\frac{\partial}{\partial x}\left(\frac{F}{m\gamma} f\right) + D\frac{\partial^{\alpha} f}{\partial |x|^{\alpha}}. \tag{2.4}$$

The Riesz fractional derivative $\partial^{\alpha}/\partial|x|^{\alpha}$ (we adopt here the notation introduced in [35]) is defined for a "sufficiently well-behaved" function $\phi(x)$ through the Liouville–Weyl derivatives [36]:

$$\frac{\mathrm{d}^{\alpha}}{\mathrm{d}|x|^{\alpha}}\phi(x) = \begin{cases} -\frac{1}{2\cos(\pi\alpha/2)}\left[D_{+}^{\alpha}\phi + D_{-}^{\alpha}\phi\right], & \alpha \neq 1, \\ -\frac{\mathrm{d}}{\mathrm{d}x} H\phi, & \alpha = 1, \end{cases} \tag{2.5}$$

where $D_{\pm}^{\alpha}$ are the left- and right-hand side Liouville–Weyl derivatives

$$D_{+}^{\alpha}\phi = \frac{1}{\Gamma(2-\alpha)}\frac{\mathrm{d}^2}{\mathrm{d}x^2}\int_{-\infty}^{x}\frac{\phi(\xi)\,\mathrm{d}\xi}{(x-\xi)^{\alpha-1}}, \quad 1 \leqslant \alpha < 2,$$

$$D_{-}^{\alpha}\phi = \frac{1}{\Gamma(2-\alpha)}\frac{\mathrm{d}^2}{\mathrm{d}x^2}\int_{x}^{\infty}\frac{\phi(\xi)\,\mathrm{d}\xi}{(\xi-x)^{\alpha-1}}, \quad 1 \leqslant \alpha < 2 \tag{2.6}$$

($D_{\pm}^{1} = \pm \mathrm{d}/\mathrm{d}x$ for $\alpha = 1$). H is the Hilbert transformation operator,

$$H\phi = \frac{1}{\pi}\int_{-\infty}^{\infty}\frac{\phi(\xi)\,\mathrm{d}\xi}{x-\xi}.$$

In Fourier space the operators of fractional derivatives have a simple form

$$\hat{\boldsymbol{\Phi}}(D_{\pm}^{\alpha}\hat{\phi}) = \int_{-\infty}^{\infty}\mathrm{d}x\exp(\mathrm{i}kx)D_{\pm}^{\alpha}\phi = (\mp\mathrm{i}k)^{\alpha}\hat{\phi}(k), \tag{2.7}$$

where $\hat{\boldsymbol{\Phi}}$ implies the Fourier transformation operation. $\hat{\phi}(k)$ is the Fourier transform of $\phi(x)$, and

$$(\mp\mathrm{i}k)^{\alpha} = |k|^{\alpha}\exp\left(\mp\frac{\alpha\pi\mathrm{i}}{2}\operatorname{sgn}k\right).$$

Since

$$\hat{\boldsymbol{\Phi}}(H\phi) = \mathrm{i}\operatorname{sgn}k\hat{\phi}, \tag{2.8}$$

then with the use of Eqs. (2.5)–(2.8) we obtain the following expression, which is valid for the Fourier transform of the Riesz fractional derivative for all α's

$$\hat{\boldsymbol{\Phi}}\left(\frac{\mathrm{d}^{\alpha}\phi}{\mathrm{d}|x|^{\alpha}}\right) = -|k|^{\alpha}\hat{\phi}. \tag{2.9}$$

In what follows, we use only the Fourier representation (2.9) for the Riesz fractional derivative.

It is worthwhile to note that the fractional generalization of ESE different from Eq. (2.4) was proposed in [37]. It is derived within the framework of the subordination of random processes which leads to the Lévy flights. In this case the stationary state is given by the Boltzmann distribution. In present paper we concentrate on the consequences of Eq. (2.4). Thus, we consider the cases which are adequately described within the Langevin approach with the Lévy noise.

If the noise term $Y(t)$ in the Langevin equation is the white Gaussian one, $\alpha = 2$, then we are in the Brownian case and Eq. (2.4) is an ordinary ESE, whose stationary solution is given by the Boltzmann formula:

$$f_{\mathrm{st}}(x) = C\exp\left(-\frac{U(x)}{k_{\mathrm{B}}T}\right), \tag{2.10}$$

where T is the temperature of the surrounding medium, and k_{B} is the Boltzmann constant. Here the Einstein relation between the intensity D of the noise and the friction coefficient γ is used:

$$D = \frac{k_{\mathrm{B}}T}{m\gamma}. \tag{2.11}$$

Thus, in the case of the Brownian oscillator the shape of the stationary PDF is dictated by the particular form of the potential energy. For the non-linear oscillators listed in Section 1 the PDFs are unimodal with their maximum at the origin. It also follows from Eq. (2.10) that for all the particular forms of the potential energy stationary PDFs decay exponentially at large values of the energy (that is, at large values of x). One could say that in case of the Gaussian noise, the form of the stationary PDF is determined by the form of the potential energy, whereas the role of the noise is only to change the width of the PDF (by varying T). As we see in the next sections, the effect of the Lévy noise ($\alpha < 2$) can be more radical.

Now we turn to another known particular case, namely, the harmonic Lévy oscillator. The potential energy function is given here by

$$U = \frac{ax^2}{2}, \tag{2.12}$$

where $a = m\omega^2$, and ω is the oscillator frequency. In dimensionless variables, $x' = x/x_0$ and $t' = t/t_0$ (where $t_0 = m\gamma/a = \gamma/\omega^2$ and $x_0 = (Dt_0)^{1/\alpha}$), Eq. (2.4) takes the form (note that we omit the prime signs)

$$\frac{\partial f}{\partial t} = \frac{\partial}{\partial x}(xf) + \frac{\partial^\alpha f}{\partial |x|^\alpha}. \tag{2.13}$$

We are interested in the stationary solution $f_{\rm st}(x)$ of Eq. (2.13). The equation for its characteristic function $\hat{f}_{\rm st}(k)$,

$$\hat{f}_{\rm st}(k) = \int_{-\infty}^{\infty} {\rm d}x\, {\rm e}^{{\rm i}kx} f_{\rm st}(x), \tag{2.14}$$

follows from Eq. (2.13) (note that we omit 'st' below):

$$\frac{{\rm d}\hat{f}}{{\rm d}k} = -{\rm sgn}\, k \cdot |k|^{\alpha-1}\hat{f}(k). \tag{2.15}$$

This equation is solved for the boundary condition

$$\hat{f}(k=0) = 1, \tag{2.16}$$

which is the consequence of normalization. The solution of Eq. (2.15) is

$$\hat{f}(k) = \exp\left(-\frac{|k|^\alpha}{\alpha}\right). \tag{2.17}$$

This is the characteristic function of the Lévy stable PDF with the index α and the scale parameter $\alpha^{-1/\alpha}$. The PDF is unimodal with a maximum being at the origin. The asymptotics at large x are determined by the first non-analytical term in the series expansion of the exponent in Eq. (2.17):

$$f(|x| \to \infty) \approx -\int_{-\infty}^{\infty} \frac{{\rm d}k}{2\pi} {\rm e}^{-{\rm i}kx} \frac{|k|^\alpha}{\alpha} = \frac{C}{|x|^{1+\alpha}}, \tag{2.18}$$

$$C = \frac{\sin(\pi\alpha/2)\Gamma(\alpha)}{\pi}.$$

In Eq. (2.18) and in the next sections we use the value of the following improper integral which is computed by the method of Abel summation [38]:

$$\int_0^\infty {\rm d}t \cdot t^{\alpha+2m} {\rm e}^{-{\rm i}t} = (-1)^{m+1} \cdot {\rm i}\, {\rm e}^{-{\rm i}(\alpha\pi/2)} \cdot \Gamma(\alpha+2m+1), \quad m = 0,1,2,\ldots \tag{2.19}$$

Thus, the stationary PDF $f(x)$ has a slowly decaying tail such that the variance $\int_{-\infty}^{\infty} x^2 f(x)\,{\rm d}x$ diverges. In the next sections we show how the properties of unimodality and long tails are modified for non-linear Lévy oscillators.

3. Quartic Lévy oscillator

In this section we deal with the quartic Lévy oscillator having the potential

$$U = \frac{bx^4}{4}. \tag{3.1}$$

3.1. Starting equations

Introducing dimensionless variables $x' = x/x_0$, $t' = t/t_0$ such that $x_0 = (m\gamma D/b)^{1/(2+\alpha)}$, $t_0 = x_0^\alpha/D$, we rewrite the FESE in dimensionless variables as (omitting primes)

$$\frac{\partial f}{\partial t} = \frac{\partial}{\partial x}(x^3 f) + \frac{\partial^\alpha f}{\partial |x|^\alpha}. \tag{3.2}$$

In order to study the properties of the stationary solution, we turn from Eq. (3.2) to the equation for the characteristic function of the stationary PDF, see Eq. (2.14):

$$\frac{{\rm d}^3\hat{f}}{{\rm d}k^3} = {\rm sgn}\, k \cdot |k|^{\alpha-1}\hat{f}(k). \tag{3.3}$$

When deriving Eq. (3.3) the natural condition is used that the characteristic function, as well as its derivatives, tends to zero at $k \to \pm\infty$. The characteristic function also obeys the following conditions:

1. $\hat{f}(0) = 1$ (normalization condition).
2. $\hat{f}(k) = \hat{f}^*(k) = \hat{f}(-k)$, where the asterisk implies complex conjugate. The first equality is a consequence of the Khintchine theorem about reality of the characteristic function for the symmetric PDF, whereas the second equality is the consequence of the Bochner–Khintchine

theorem about positive definiteness of the characteristic function.

3. Since the integer moments of the PDF (if they exist) are connected with the derivatives of the characteristic function at $k = 0$ through

$$\langle x^p \rangle = \frac{1}{\mathrm{i}^p} \frac{\mathrm{d}\hat{f}^{(p)}(0)}{\mathrm{d}k^p}, \quad p = 1, 2 \ldots$$

then

$$\frac{\mathrm{d}\hat{f}^{(p)}(0)}{\mathrm{d}k^p} = 0, \quad p = 1, 3, 5, \ldots,$$

because the PDF is a symmetric function, and hence, all odd moments are equal to zero. Conditions (3.1)–Eq. (3.24) are valid for those odd p, for which the pth moments of the PDF exist.

3.2. Stationary solution for quartic Cauchy oscillator

In the particular case of the Cauchy oscillator, $\alpha = 1$, the solution of Eq. (3.3) is

$$\hat{f}(k) = \frac{2}{\sqrt{3}} \exp\left(-\frac{|k|}{2}\right) \cdot \cos\left(\frac{\sqrt{3}|k|}{2} - \frac{\pi}{6}\right). \tag{3.4}$$

By an inverse Fourier transformation, we obtain the stationary PDF for the quartic Cauchy oscillator

$$f(x) = \frac{1}{\pi(1 - x^2 + x^4)}. \tag{3.5}$$

Note that $f(x)$ has two important properties:

1. Power-tail asymptotics at $x \to \pm\infty : f(x) \propto x^{-4}$, hence, the *variance is finite*.
2. Bimodal structure of the PDF: it has a local minimum at $x_{\min} = 0$ and two maxima at $x_{\max} = \pm 1/2$.

These properties are drastically different from the properties of the stationary solutions for both the Brownian quartic oscillator and the linear Lévy oscillator. Below we see that the steep power-law asymptotics and the bimodality are inherent for the solutions with all α's such that $1 \leqslant \alpha < 2$.

3.3. Asymptotics of the characteristic function at large values of the argument

Now return to Eq. (3.3) and consider the asymptotics of the solution at $k \to \infty$. For this purpose, we pass to the equation for the function

$$\eta(\xi) = k^{(\alpha-1)/3} \hat{f}(k), \quad \xi = k^{(\alpha+2)/3}. \tag{3.6}$$

The function $\eta(\xi)$ obeys the equation

$$\frac{\mathrm{d}^3\eta}{\mathrm{d}\xi^3} + \frac{A}{\xi^2}\left(\frac{\mathrm{d}\eta}{\mathrm{d}\xi} - \frac{\eta}{\xi}\right) = \lambda\eta, \tag{3.7}$$

where $A = (\alpha - 1)(\alpha + 5)(\alpha + 2)^{-2}$, $\lambda = (3/(\alpha + 2))^3$. We are interested in asymptotics of $\eta(\xi)$ at $\xi \to \infty$. The equations of this type are considered in [39] together with the method of finding asymptotics. Following this method, we find asymptotics of the form:

$$\eta(\xi) = u(\xi)\mathrm{e}^{\beta\xi}. \tag{3.8}$$

Inserting Eq. (3.8) into Eq. (3.7) we get the equation for u

$$\frac{\mathrm{d}^3u}{\mathrm{d}\xi^3} + 3\beta\frac{\mathrm{d}^2u}{\mathrm{d}\xi^2} + \left(3\beta^2 + \frac{A}{\xi^2}\right)\frac{\mathrm{d}u}{\mathrm{d}\xi} + \left(\beta^3 - \lambda - \frac{A}{\xi^3}\right)u = 0. \tag{3.9}$$

The characteristic equation takes on the form

$$\beta^3 = \lambda, \tag{3.10}$$

thus the term of the zeroth order in $1/\xi$ in the coefficient of u is equal zero. Now, the solution of Eq. (3.9) is taking on the form

$$u = c_0 + \frac{c_1}{\xi} + \frac{c_2}{\xi^2} + \cdots, \tag{3.11}$$

where c_0 is an arbitrary constant. Inserting Eq. (3.11) into Eq. (3.9) we obtain $c_1, c_2, \ldots$ in terms of c_0. The result is

$$u = c_0\left(1 - \frac{A}{6\beta^2\xi^2} - \frac{A}{6\beta^3\xi^3} + \cdots\right). \tag{3.12}$$

From the roots of Eq. (3.10) one has to take those which exhibit a negative real part. Note, that if we take only the first term in the expansion (3.12), then the exponential solution for $\eta(\xi)$ can be obtained directly from Eq. (3.7) by retaining only the third order derivative in the left-hand side. As the result we get

$$\eta(\xi) = C\exp\left(-\frac{3}{2(\alpha+2)}\xi\right)\cos\left(\frac{3\sqrt{3}}{2(\alpha+2)}\xi - \Theta\right), \tag{3.13}$$

where C and θ are arbitrary constants. The result depends on two unknown constants since we use the boundary condition at infinity, only. Now we return to the characteristic function by using Eq. (3.6), and find

$$f(k) = Ck^{-(\alpha-1)/3}\exp\left(-\frac{3k^{(\alpha+2)/3}}{2(\alpha+2)}\right) \cdot\cos\left(\frac{3\sqrt{3}k^{(\alpha+2)/3}}{2(\alpha+2)} - \Theta\right). \tag{3.14}$$

It follows from Eq. (3.14) that the function $\hat{f}(k)$ oscillates and tends to zero at $k\to\infty$ exponentially. We can check this formula for two particular cases, $\alpha = 1$ and 2.

1. Cauchy oscillator, $\alpha = 1$.

By comparing Eqs. (3.14) and (3.4) we get $C = 2/3^{1/2}$, $\theta = \pi/6$.

2. Brownian oscillator, $\alpha = 2$.

We explore the asymptotics of the following integral at large k's:

$$\int_{-\infty}^{\infty} \mathrm{d}x\cdot\exp\left(\mathrm{i}kx - x^{2m}\right) = \left(\frac{\pi}{m(2m-1)}\right)^{1/2}(2m)^{(m-1)/(2m-1)}\cdot k^{-(m-1)/(m-2)} \cdot\exp\left(c_m k^{2m/(2m-1)}\cdot\cos\frac{\pi m}{2m-1}\right) \times\cos\left(c_m x^{2m/(2m-1)}\sin\frac{\pi m}{2m-1} - \frac{\pi(m-1)}{2(2m-1)}\right),$$

$$c_m = \frac{2m-1}{2m}(2m)^{-1/(2m-1)}.$$

With the help of this formula we have, for the Brownian quartic oscillator,

$$\hat{f}(k) = \int_{-\infty}^{\infty}\mathrm{d}x f(x)\exp(\mathrm{i}kx) \approx \frac{2^{10/3}\sqrt{3\pi}}{\Gamma(1/4)}|k|^{-1/3}\exp\left(-\frac{3}{8}|k|^{4/3}\right) \times\cos\left(\frac{3\sqrt{3}}{8}|k|^{4/3} - \frac{\pi}{6}\right).$$

By comparing with Eq. (3.14) we get

$$C = \frac{2^{10/3}\sqrt{3\pi}}{\Gamma(1/4)}, \quad \theta = \frac{\pi}{6}.$$

3.4. Series expansion of the characteristic function at small values of the argument

We return to Eq. (3.7) and construct the solution in the form of a series in positive powers of ξ. We look for the particular solution η_μ of Eq. (3.7) in the form

$$\eta_\mu = \xi^\mu\sum_{j=0}^{\infty} a_j^{(\mu)}\xi^{3j}. \tag{3.15}$$

The exponent μ is defined as follows. Denoting by $\hat{L}$ the operator on the left-hand side of Eq. (3.7), we find

$$\hat{L}\xi^m = \xi^{m-3}\{m(m-1)(m-2) + A(m-1)\}. \tag{3.16}$$

Equating the terms in the parenthesis to zero we get three roots giving three values of μ in Eq. (3.15):

$$\mu_0 = 1, \quad \mu_+ = \frac{\alpha+5}{\alpha+2}, \quad \mu_- = \frac{\alpha-1}{\alpha+2}. \tag{3.17}$$

The three roots (3.17) determine three particular solutions of Eq. (3.7). Inserting Eq. (3.15) into Eq. (3.7) we get the recurrent relation between $a_j^{(\mu)}$'s:

$$a_{j+1}^{(\mu)}(\mu+3j+2)[(\mu+3j+3)(\mu+3j+1)+A] = \lambda a_j^{(\mu)}. \tag{3.18}$$

The three series contain arbitrary constants $a_0^{(\mu)}$, which have to be determined using boundary conditions. With Eqs. (3.15), (3.17) and (3.6) we pass to the functions

$$\hat{f}_\mu(\xi) = \eta_\mu(\xi)\xi^{-\mu_-} = \xi^{\mu-\mu_-}\sum_{j=0}^{\infty} a_j^{(\mu)}\xi^{3j}, \tag{3.19}$$

where μ is equal to μ_0, μ_+ or μ_-. These are the expressions for the three particular solutions for the characteristic function. It follows immediately from the normalization condition $\hat{f}(\xi=0) = 1$ that $a_0^{(\mu_-)} = 1$. Thus, we have to determine $a_0^{(\mu_0)}$ and $a_0^{(\mu_+)}$ only. Note that, since $\mu_0 - \mu_- - 1 < 0$, from the condition $\hat{f}'(\xi=0) = 0$ we have $a_0^{(\mu_0)} = 0$.

Therefore, only one constant, $a_0^{(\mu_+)}$, remains unknown, and the general solution is

$$\hat{f}(\xi) = \sum_{j=0}^{\infty} a_j^{(\mu_-)} \xi^{3j} + \xi^{6/(\alpha+2)} \sum_{j=0}^{\infty} a_j^{(\mu_+)} \xi^{3j}, \qquad (3.20)$$

where $a_j^{(\mu_\pm)}$ are determined by Eq. (3.18), and $a_0^{(\mu_-)} = 1$. Turning to the variable k instead of ξ, and changing notations slightly we get

$$\hat{f}(k) = \Sigma_1 + ak^2\Sigma_2, \qquad (3.21)$$

where

$$\Sigma_1 = \sum_{j=0}^{\infty} a_j^{(\mu_-)} k^{j(\alpha+2)},$$
$$\Sigma_2 = \sum_{j=0}^{\infty} a_j^{(\mu_+)} k^{j(\alpha+2)}, \qquad (3.22)$$

and $a_j^{(\mu_\pm)}$ are determined by Eq. (3.18) with $a_0^{(\mu_-)} = a_0^{(\mu_+)} = 1$, whereas $\mu_\pm$ are determined by Eq. (3.17). In order to define a, we use the boundary condition at infinity, $\hat{f}(k = \infty) = 0$, that is

$$a = -\lim_{k\to\infty} \frac{\Sigma_1}{k^2\Sigma_2}. \qquad (3.23)$$

Therefore, in spite of the fact that the particular solutions Σ_1 and $k^2\Sigma_2$ grow at infinity, we chose their linear combination, which tends to zero at $k \to \infty$. The possibility of this choice is confirmed by the results of a numerical analysis, which are shown below.

In Fig. 1 the properties of particular solutions for the quartic Lévy oscillator are shown for $\alpha = 1.5$. In Fig. 1(a), the two solutions, Σ_1 and $k^2\Sigma_2$, are depicted versus k. Both particular solutions grow to infinity at $k \to \infty$, however, their ratio $a(k) = -\Sigma_1(k)/k^2\Sigma_2(k)$ tends to the constant value equal to a_0. This fact is illustrated in Fig. 1(b), in which the difference $|a(k) - a_0|$ is shown versus k in a semi-logarithmic scale. The value of $a(k)$ oscillates and converges to a_0; a_0 is defined as $a_0 \equiv a(15) = -0.384411398$.

To construct the characteristic function numerically, we use the solution (3.21), (3.22), which is continued with the asymptotics (3.14) for large k. This continuation method is explained in Fig. 2 for $\alpha = 1.5$. In Eq. (3.14) we set $\theta = \pi/6$ (as in cases $\alpha = 1$ and 2), whereas C is determined by equating both solutions, Eqs. (3.21) and (3.14), in the point of the first minimum of the characteristic function (dotted vertical line). The solid line indicates the solution given by the series (3.21), (3.22) with $a = a_0 = a(15)$, the dotted line indicates large k asymptotics (3.14). It is seen from Fig. 2(b) that for such a choice of C and θ the period and the phase of oscillations of $\hat{f}(k)$ coincide with good accuracy. In particular, we are able to make a comparison between the positions of zeros of $\hat{f}(k)$ estimated by using the asymptotics and the series. It appears that they coincide with the accuracy 10^{-3}–10^{-4}.

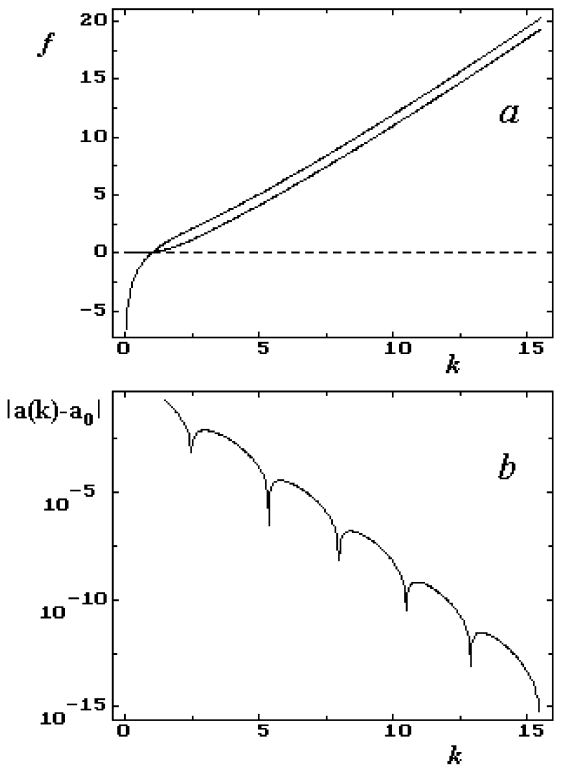

Fig. 1. Properties of the particular solutions Σ_1 and $k^2\Sigma_2$, see Eqs. (3.21), (3.22): (a) both solutions as the functions of k, $\alpha = 1.5$; (b) the difference $|a(k) - a_0|$ versus k. For the notations $a(k)$ and a_0 see Section 3.

Now we consider two important properties which have been already discussed for the particular case of the Cauchy oscillator, namely, power-law tails and bimodality. Consider power-law tails

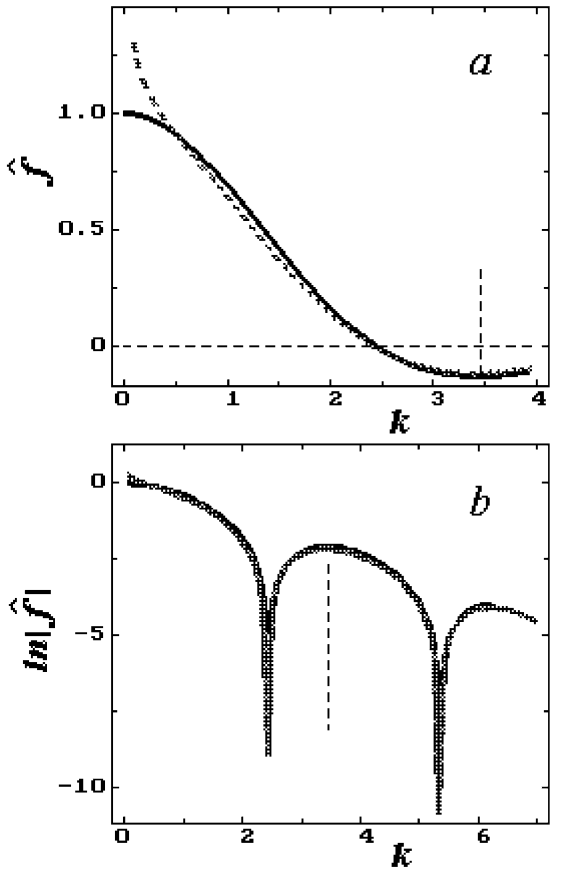

Fig. 2. Illustration of the continuation method for numerical construction of the characteristic function, $\alpha = 1.5$. Solid lines indicate the solution in the form of a series (3.21)–(3.23) in (a) linear scale, and (b) semi-logarithmic scale. Dotted lines indicate the asymptotics (3.14) with $\theta = \pi/6$, and C determined from the condition of coincidence of the expressions given by Eqs. (3.14) and (3.21) in the location of the first minimum. See Section 3 for more details.

at $x \to \pm\infty$ at first. These asymptotics are determined by the first non-analytical term in Eq. (3.21), that is, the term $a_1^{(\mu_-)}|k|^{\alpha+2}$. By making an inverse Fourier transformation of this term, we get, with using Eq. (2.17),

$$f(x) \approx \frac{\sin(\pi\alpha/2)\Gamma(\alpha)}{\pi|x|^{\alpha+3}}, \quad x \to \pm\infty. \tag{3.24}$$

It follows from Eq. (3.24) that the equilibrium PDF has a power-law tail, $f(x) \propto |x|^{-(\alpha+3)}$, and, thus the variance is finite. This behavior is strikingly different from that of a non-linear Brownian oscillator and of linear Lévy oscillator. The "long tails" can be explained qualitatively, if we turn to the Langevin description of the Lévy oscillator. The Langevin approach relevant to the FESE implies that the non-linear overdamped oscillator is influenced by "white Lévy noise" $Y(t)$, whose PDF behaves as $|Y|^{-1-\alpha}$ at $|Y| \to \infty$. These "long tails" cause that the large absolute values of the noise occur frequently, which, in turn, lead to large increments of the coordinate. However, it is also clear that the PDF of the coordinate x must fall off more rapidly at $x \to \infty$ than the PDF of the noise Y, because of the presence of the potential well, which prevents from escaping to regions far off the origin.

In Fig. 3 the stationary PDF is shown by solid lines in a linear (at the top) and semi-logarithmic

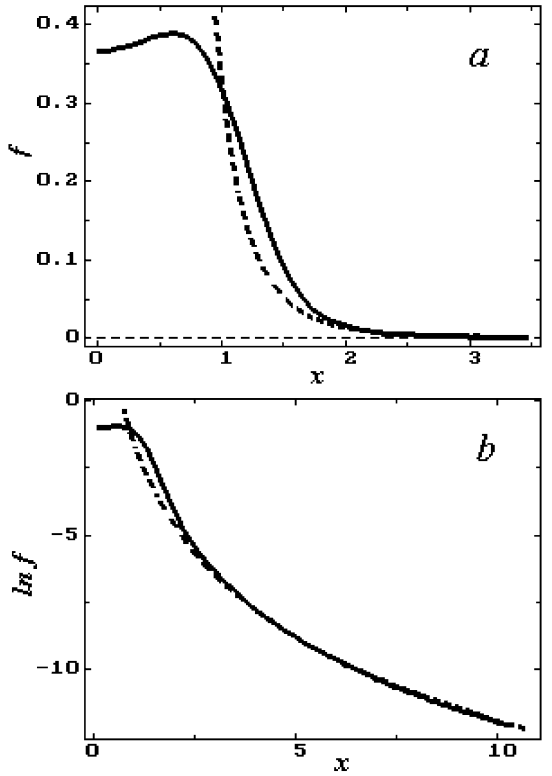

Fig. 3. Solid lines: stationary PDFs for the quartic oscillator in (a) linear scale, and (b) semi-logarithmic scale, $\alpha = 1.5$. Dotted lines: power-law asymptotics (3.24).

(at the bottom) scales. The PDF is obtained by an inverse Fourier transformation of the characteristic function shown in Fig. 2, $\alpha = 1.5$. The dashed lines indicate asymptotics (3.24). One can see, especially from the semi-logarithmic plot, that the asymptotics is a good approximation beginning from k equal to ~ 2. In this figure the second important property, namely, bimodality is clearly seen on a linear scale. In Fig. 4 the profiles of stationary PDFs (obtained by an inverse Fourier transformation) are shown for the different Lévy indices from $\alpha = 1$ at the top of the figure up to $\alpha = 2$ at the bottom. It is seen that the bimodality is most strongly expressed for $\alpha = 1$. With the Lévy index increasing, the bimodal profile smoothes out, and, finally, it turns to a unimodal one at $\alpha = 2$, that is, for the Boltzmann distribution.

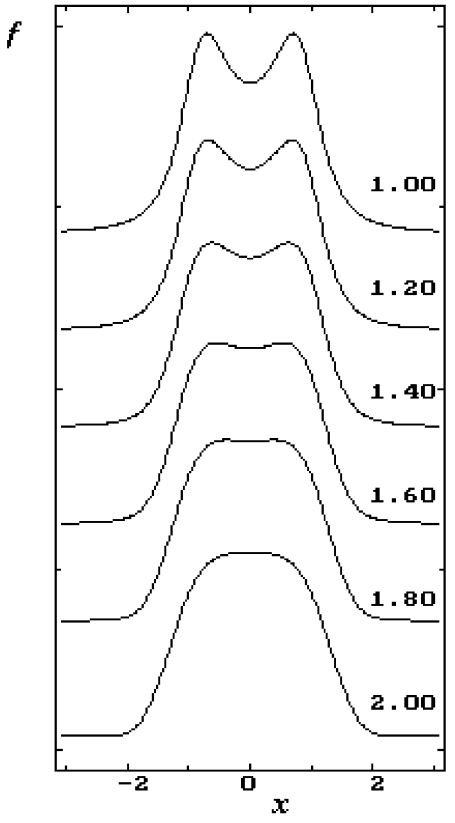

Fig. 4. Profiles of stationary PDFs of the quartic oscillator for different Lévy indices, from $\alpha = 1$ (at the top) till $\alpha = 2$ (at the bottom).

4. Anharmonic Lévy oscillator

In the previous sections we have seen that in a linear force field $F(x)$, the harmonic Lévy oscillator, the stationary PDF is unimodal, whereas in the quartic case the bimodal stationary PDF arises. In this section, we show the transition from unimodal to bimodal stationary PDFs, as the parameters of the oscillator are changed. The anharmonic Lévy oscillator with the potential energy function

$$U = \frac{ax^2}{2} + \frac{bx^4}{4}, \quad a \geqslant 0 \tag{4.1}$$

is considered.

4.1. Bimodal–unimodal transition for anharmonic Cauchy oscillator

Introducing the same dimensionless variables as in the previous sections, and setting $a' = at_0/m\gamma$ we obtain, again omitting primes:

$$\frac{\partial f}{\partial t} = a\frac{\partial}{\partial x}(xf) + \frac{\partial}{\partial x}(x^3 f) + \frac{\partial^\alpha f}{\partial |x|^\alpha}. \tag{4.2}$$

Note that in dimensionless variables we deal with the potential energy function

$$U = \frac{ax^2}{2} + \frac{x^4}{4}, \tag{4.3}$$

thus, only one parameter, a, remains. The stationary characteristic function obeys the equation

$$\frac{\mathrm{d}^3 \hat{f}(k)}{\mathrm{d}k^3} - a\frac{\mathrm{d}\hat{f}}{\mathrm{d}k} = \operatorname{sgn} k |k|^{\alpha-1}\hat{f}(k). \tag{4.4}$$

We solve this equation for the Cauchy case, $\alpha = 1$, on the right semi-axis with the boundary conditions

$$\hat{f}(0) = 1, \quad \frac{\mathrm{d}\hat{f}(0)}{\mathrm{d}k} = 0, \quad \hat{f}(k = \infty) = 0. \tag{4.5}$$

The solution is

$$\hat{f}(k) = \frac{1}{z - z^*}\left(-z^* \mathrm{e}^{zk} + z\mathrm{e}^{z^* k}\right), \tag{4.6}$$

where z is the complex root of the characteristic equation

$$z^3 - az - 1 = 0, \tag{4.7}$$

that is

$$z = -\frac{u+w}{2} + i\sqrt{3}\frac{u-w}{2}, \tag{4.8}$$

where

$$u^3 = \frac{1}{2}\left(1 + \sqrt{1 - \frac{4a^3}{27}}\right),$$
$$w^3 = \frac{1}{2}\left(1 - \sqrt{1 - \frac{4a^3}{27}}\right). \tag{4.9}$$

We are interested in the unimodal–bimodal transition when the parameter a varies. Let a_c be the critical value, which we determine by using Eqs. (4.6)–(4.9). The condition for the transition is

$$\left.\frac{d^2 f}{dx^2}\right|_{x=0} = 0, \tag{4.10}$$

or equivalently, defining

$$J(a) = \int_0^\infty dk\, k^2 \hat{f}(k), \tag{4.11}$$

$$J(a_c) = 0. \tag{4.12}$$

If $J > 0$ the stationary PDF is unimodal; if $J < 0$, it is bimodal. Inserting Eq. (4.6) into Eq. (4.11) we get

$$J = -2\frac{(z+z^*)(z^2+z^{*2})}{|zz^*|^3}, \tag{4.13}$$

and, thus

$$\mathrm{sgn} J = \mathrm{sgn}\,(z^2 + z^{*2}). \tag{4.14}$$

Inserting Eqs. (4.8), (4.9) into Eq. (4.14) we find

$$\mathrm{sgn} J = -\mathrm{sgn}\left(u^2 + w^2 - \frac{4}{3}a\right). \tag{4.15}$$

Defining $\zeta \equiv 4^{1/3} a_c/3$, we get from Eq. (4.15)

$$4\zeta = \left(1 + \sqrt{1-\zeta^3}\right)^{2/3} + \left(1 - \sqrt{1-\zeta^3}\right)^{2/3}. \tag{4.16}$$

The solution of Eq. (4.16) is $\zeta = 0.419974$ and therefore

$$a_c = 0.793701. \tag{4.17}$$

For $a > a_c$ the quadratic term in the potential energy function prevails, and the stationary PDF has one maximum at the origin. In contrast, for $a < a_c$ the quartic term dominates and dictates the shape of the PDF. As a result the bimodal stationary PDF appears with the local minimum at the origin.

In Fig. 5 the profiles of the stationary PDFs (obtained by an inverse Fourier transformation) are shown for the anharmonic Cauchy oscillator for different values of the coefficient a of Eq. (4.1), from top to bottom: $a = 0$, 0.2, 0.4, 0.6, and 0.8. The PDFs are obtained by inverse Fourier transformation of the characteristic functions (4.6). It is clear that the bimodality is most pronounced for $a = 0$, that is, for the quartic Cauchy oscillator. As the parameter a increases the bimodal profile smoothes out, and, finally, it turns to a unimodal one. It is interesting to note the similarity between Figs. 4 and 5. However, of course, their meaning is quite different.

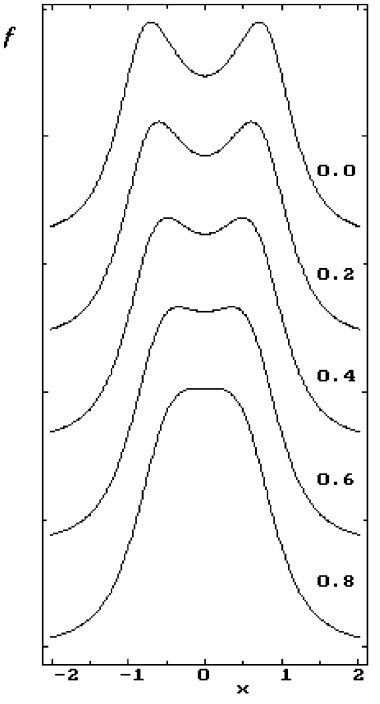

Fig. 5. Profiles of stationary PDFs of the anharmonic Cauchy oscillator for different values of the parameter a in the potential energy function, Eq. (4.3), from top to bottom: $a = 0, 0.2, 0.4, 0.6$, and 0.8.

4.2. Bimodal–unimodal transition for anharmonic Lévy oscillator

For more general cases different from $\alpha = 1$ we start from Eq. (4.4) for $k \geqslant 0$. Using the transformation

$$\eta(\xi) = k^{(x-1)/3}\hat{f}(k), \quad \xi = k^{(x+1)/3}, \tag{4.18}$$

we get an equation for $\eta(\xi)$:

$$\eta''' - \lambda\eta + a\lambda^{2/3}\left(\eta' - \tilde{v}\frac{\eta}{\xi}\right)\xi^{-2\tilde{v}} + \frac{A}{\xi^2}\left(\eta' - \frac{\eta}{\xi}\right) = 0, \tag{4.19}$$

where

$$\tilde{v} = \frac{\alpha - 1}{\alpha + 2}, \quad A = \frac{(\alpha - 1)(\alpha + 5)}{(\alpha + 2)^2} = \tilde{v}\frac{\alpha + 5}{\alpha + 2},$$
$$\lambda = \left(\frac{3}{2 + \alpha}\right)^3. \tag{4.20}$$

In the analysis presented below we assume that

$$\tilde{v} \ll 1, \tag{4.21}$$

thus, we consider Lévy indices which are close to $\alpha = 1$. However, we note that the maximum value of $\tilde{v}$ for $\alpha = 2$ is $\tilde{v}_{\max} = 0.25$, which is also less than unity. So, we expect that our consideration is valid (at least, qualitatively) over the whole region of α values. Condition (4.21) allows to simplify the equation for $\eta(\xi)$. Indeed, assuming that $\xi \gg \tilde{v}^{1/3}$ we can neglect the last term (containing the parameter A) in the left-hand side of Eq. (4.19) relative to the term $-\lambda\eta$. On the other hand, assuming $\xi \ll \exp(1/\tilde{v})$, we may neglect the factor $\xi^{-2\tilde{v}}$. Therefore, within the interval

$$\tilde{v} \ll \xi \ll \mathrm{e}^{1/\tilde{v}} \tag{4.22}$$

we can consider the following equation instead of Eq. (4.19):

$$\eta''' - a\lambda^{2/3}\eta' = \lambda\eta. \tag{4.23}$$

The solution of Eq. (4.23) is

$$\eta(\xi) = \frac{1}{z - z^*}\left(z\mathrm{e}^{z^*\xi} - z^*\mathrm{e}^{z\xi}\right), \tag{4.24}$$

where z is the complex root of the characteristic equation (compare with Eq. (4.7))

$$z^3 - a\lambda^{2/3}z - \lambda = 0, \tag{4.25}$$

that is,

$$z = -\frac{u + w}{2} + \mathrm{i}\frac{\sqrt{3}}{2}(u - w), \tag{4.26}$$

where

$$u = \left(\frac{\lambda}{2}\right)^{1/3}\left(1 + \sqrt{1 - \frac{4a^3}{27}}\right)^{1/3},$$
$$w = \left(\frac{\lambda}{2}\right)^{1/3}\left(1 - \sqrt{1 - \frac{4a^3}{27}}\right)^{1/3}. \tag{4.27}$$

Following the method described in Section 4.1, we are interested in the sign of

$$J = \int_0^\infty \mathrm{d}k \cdot k^2\hat{f}(k)$$
$$= \frac{3}{\alpha + 2}\int_0^\infty \mathrm{d}\xi \cdot \xi^\mu\eta(\xi), \tag{4.28}$$

where $\mu = (8 - 2\alpha)/(\alpha + 2)$. Inserting the solution (4.24) into Eq. (4.28) we get

$$J = \frac{3\Gamma(\mu + 1)}{(\alpha + 2)\,\mathrm{Im}\,z \cdot |z|^\mu}\sin[(\mu + 2)(\pi - \varphi)], \tag{4.29}$$

where $\varphi = \arg(z)$. When deriving Eq. (4.29), we use the following subsidiary integral:

$$\int_0^\infty \mathrm{d}\xi \cdot \xi^\mu \mathrm{e}^{z\xi} = \frac{\mathrm{e}^{\mathrm{i}\,\pi(\mu+1)}}{z^{\mu+1}}\Gamma(\mu + 1).$$

Since

$$\mathrm{sgn}J = \mathrm{sgn}\{\sin[(\mu + 2)(\pi - \varphi)]\}, \tag{4.30}$$

the critical value a_c, for which the bimodal–unimodal transition occurs, is determined from the equation

$$\sin[(\mu + 2)(\pi - \varphi)] = 0, \tag{4.31}$$

or

$$(\mu + 2)(\pi - \varphi) = l\pi, \quad l = 0, 1, 2, \ldots \tag{4.32}$$

What value of l must be chosen? We first note that $l = 0$ corresponds to the degenerate case $u = w$. At $l = 2$ and $\alpha = 1$ we get $\varphi(l = 2) \equiv \varphi_2 = \pi/2$, which is also invalid, since the real part of z must be negative. Therefore, we choose $l = 1$, and

$$\varphi_1 \equiv \varphi(l = 1) = \frac{\pi}{12}(10 - \alpha). \tag{4.33}$$

On the other hand, it follows from Eqs. (4.26) and (4.27) that

$$\cos\varphi_1 = -\frac{u+w}{2\sqrt{u^2+w^2-uw}}. \tag{4.34}$$

Since

$$uw = -\frac{\lambda^{2/3}}{3}a_c, \tag{4.35}$$

we get from Eqs. (4.34) and (4.35):

$$u^2+w^2 = \frac{2}{3}\lambda^{2/3}a_c\frac{1+2\cos^2\varphi_1}{4\cos^2\varphi_1-1}. \tag{4.36}$$

Denoting $\zeta = 4^{1/3}a_c/3$, and inserting Eqs. (4.27) into Eq. (4.36) we get

$$\left(1+\sqrt{1-\zeta^3}\right)^{2/3}+\left(1-\sqrt{1-\zeta^3}\right)^{2/3} = 2\zeta\frac{1+2\cos^2\varphi_1}{4\cos^2\varphi_1-1}. \tag{4.37}$$

Eq. (4.37) defines the value of a_c of the parameter a for which the bimodal–unimodal transition occurs. In the particular case $\alpha = 1$ Eq. (4.37) is reduced to Eq. (4.16).

Eq. (4.37) is solved numerically, and the results are shown in Fig. 6 on the plane (α–a). The stationary states with the unimodal PDFs are above the curve obtained from the equation. The region marked in gray indicates the stationary states with the bimodal PDFs. Since $a_c < 1$, one could say that the bimodal states occur if the non-linear effects are strong, not being just small corrections to the linear harmonic term. In other words, the bimodality is the effect of a strong non-linearity of the force field. Small anharmonic corrections to the linear problem do not lead to the change of the unimodal shape of stationary PDF for the linear Lévy oscillator which is in itself remarkable.

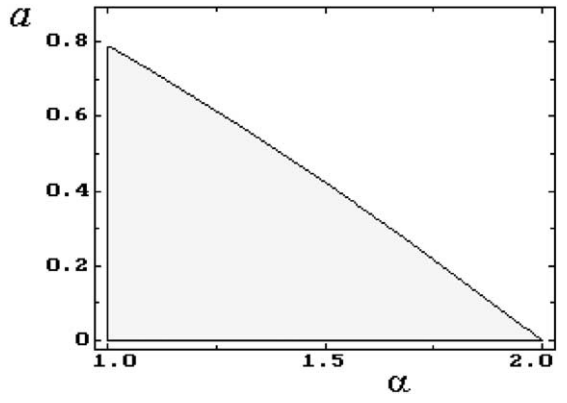

Fig. 6. Regions of unimodal and bimodal stationary states for the anharmonic Lévy oscillator on the (α–a) plane. The domain of the parameters (α, a), for which the stationary PDFs have two humps is indicated in gray.

5. Strongly non-linear Lévy oscillator

In this section we study stationary solutions for the non-linear Lévy oscillator with the potential energy function

$$U = \frac{bx^{2m+2}}{2m+2}, \quad m = 0,1,2\ldots \tag{5.1}$$

Choosing dimensionless variables $x' = x/x_0$, $t' = t/_0$ such that $x_0 = (m\gamma D/b)^{1/(2m+\alpha)}$, $t_0 = x_0^\alpha/D$, we obtain the kinetic equation in dimensionless variables (omitting primes)

$$\frac{\partial f}{\partial t} = \frac{\partial}{\partial x}\left(x^{2m+1}f\right)+\frac{\partial^\alpha f}{\partial|x|^\alpha}. \tag{5.2}$$

As before, we pass to the characteristic function of the stationary PDF and consider the solution of the equation following from Eq. (5.2):

$$\frac{\mathrm{d}^{2m+1}}{\mathrm{d}k^{2m+1}}\hat{f}(k) = (-1)^{m+1}\operatorname{sgn}k|k|^{\alpha-1}\hat{f}(k) \tag{5.3}$$

with the boundary conditions

$$\hat{f}(\pm\infty) = 0, \quad \hat{f}(0) = 1, \quad \hat{f}'(0) = \hat{f}^{(3)}(0) = \cdots = \hat{f}^{(2m-1)}(0) = 0. \tag{5.4}$$

We look for the solutions of Eq. (5.3) at $k \geqslant 0$ in the form

$$\hat{f}(k) = \varphi_0(k)+\sum_{j=1}^{\infty}k^{vj}\varphi_j(k), \tag{5.5}$$

where φ_0, φ_j are analytical functions, and v is a non-integer positive number (if $\alpha \neq 1,2$). After inserting Eq. (5.5) into Eq. (5.3) there are no terms containing integer powers of k in the right-hand side, thus the condition $\varphi_0^{(2m+1)}(k) = 0$ is fulfilled, and $\varphi_0(k)$ is the polynomial of order not higher than $2m$.

Further, since all the odd derivatives of $\hat{f}(k)$ (if they exist) are equal to zero at $k = 0$, the polynomial φ_0 contains even powers of k only,

$\varphi_0 \equiv \varphi_0(k^2)$. We show that $\varphi_j(k)$ are also polynomials whose order is not higher than $2m$, and which contain even powers of $k$only, $\varphi_j \equiv \varphi_j(k^2)$. For this purpose we insert Eq. (5.5) into Eq. (5.3) and use the following relations:

$$\frac{\mathrm{d}^{2m+1}}{\mathrm{d}k^{2m+1}} k^{vj} \varphi_j(k) = \sum_{p=0}^{2m+1} C_{2m+1}^{p} \frac{\mathrm{d}^p \varphi_j(k)}{\mathrm{d}k^p} \frac{\mathrm{d}^{2m+1-p}}{\mathrm{d}k^{2m+1-p}} k^{vj},$$

and

$$\frac{\mathrm{d}^{2m+1-p}}{\mathrm{d}k^{2m+1-p}} k^{vj} = vj(vj-1)\cdots(vj-(2m-p)) \times k^{vj-(2m+1)+p}.$$

As a result we obtain

$$\sum_{j=1}^{\infty} \sum_{p=0}^{2m+1} C_{2m+1}^{p} k^p \frac{\mathrm{d}^p \varphi_j(k)}{\mathrm{d}k^p} vj \times (vj-1)\cdots(vj-2m+p) k^{vj-(2m+1)} = (-1)^{m+1} k^{\alpha-1} \varphi_0(k^2) + (-1)^{m+1} \times \sum_{j=1}^{\infty} k^{vj+\alpha-1} \varphi_j(k). \tag{5.6}$$

After equating the terms with the same powers of k we get

$$v = \alpha + 2m, \tag{5.7}$$

and

$$\sum_{p=0}^{2m+1} C_{2m+1}^{p} k^p \frac{\mathrm{d}^p \varphi_j(k)}{\mathrm{d}k^p} j(\alpha+2m)[j(\alpha+2m)-1]\cdots [j(\alpha+2m)-2m+p] = (-1)^{m+1} \varphi_{j-1}(k). \tag{5.8}$$

It follows from Eq. (5.8) that since φ_0 is a polynomial of k^2 of order not higher than m, then all φ_j's are also polynomials of k^2 of order not higher than m.

Writing φ_j as

$$\varphi_j(k^2) = \sum_{l=1}^{m} a_j^{(l)} k^{2l}, \quad j = 0, 1, \ldots \tag{5.9}$$

($a_0^{(0)} = 1$ due to $\hat{f}(0) = 1$), and inserting Eq. (5.9) into Eq. (5.5) we get

$$\hat{f}(k) = \sum_{l=0}^{m} k^{2l} \left(a_0^{(l)} + \sum_{j=1}^{\infty} a_j^{(l)} k^{j(\alpha+2m)} \right). \tag{5.10}$$

The general solution is the superposition of the particular solutions of the form

$$k^{2l} \left(1 + \sum_{j=1}^{\infty} \tilde{a}_j^{(l)} k^{j(\alpha+2m)} \right), \tag{5.11}$$

where $\tilde{a}_j^{(l)} = a_j^{(l)} / a_0^{(l)}$, $l = 0, \ldots, m$.

The coefficients $\tilde{a}_j^{(l)}$ are defined after inserting Eq. (5.11) into Eq. (5.6)

$$\tilde{a}_j^{(l)}[j(\alpha+2m)+2l][j(\alpha+2m)+2l-1]\cdots [j(\alpha+2m)-2(m-l)] = \tilde{a}_{j-1}^{(l)}(-1)^{m+1}, \quad j = 1, 2, \ldots, \tilde{a}_0^{(l)} = 1. \tag{5.12}$$

Eqs. (5.11) and (5.12) completely define the set of m particular solutions of Eq. (5.3). One may convince oneself that the results for the linear and quartic Lévy oscillators follow immediately from Eqs. (5.11) and (5.12).

Consider the asymptotics of stationary PDFs at $|x| \to \infty$. They are determined by the non-analytical term containing the smallest power of k in Eq. (5.5), that is, the term

$$a_1^{(0)} k^{\alpha+2m}. \tag{5.13}$$

Making an inverse Fourier transformation and using Eq. (2.19) we get

$$f(x) \approx \frac{C_\alpha}{|x|^{\alpha+2m+1}}, \quad |x| \to \infty, \tag{5.14}$$

where

$$C_\alpha = \frac{\Gamma(\alpha)\sin(\pi\alpha/2)}{\pi}.$$

It follows from Eq. (5.13) that moment of the order greater than $2m+1$ diverges. It is also worthwhile to note that C_α does not depend on m. The variance however is finite which means that the potential in Eq. (5.1) confines Lévy noise of index α.

6. Numerical simulation

We carry out numerical modeling based on the solution of the Langevin equation, Eq. (2.1), on a time grid t_0, $t_1, \ldots, t_n, \ldots$, with a time step δt, $t_0 = 0$, $t_n = n\delta t$:

$$x_{n+1} = x_n + F(x_n)\delta t + (\delta t)^{1/\alpha} Y_1(n\delta t), \tag{6.1}$$

where $F(x_n)$ is the (dimensionless) force field at the point x_n, $Y_1(0)$, $Y_1(\delta t)$, $Y_1(2\delta t),\ldots,Y_1(n\delta t),\ldots \equiv \{Y_1\}$ is a discrete-time approximation to a white Lévy noise with a unit scale parameter, that is, the sequence of independent random variables possessing the characteristic function

$$\hat{p}(k) = \exp(-|k|^{\alpha}). \tag{6.2}$$

One of the possible methods for generating the sequence $\{Y_1\}$ is described in [40]. The results of numerical modeling are presented in Figs. 7–10.

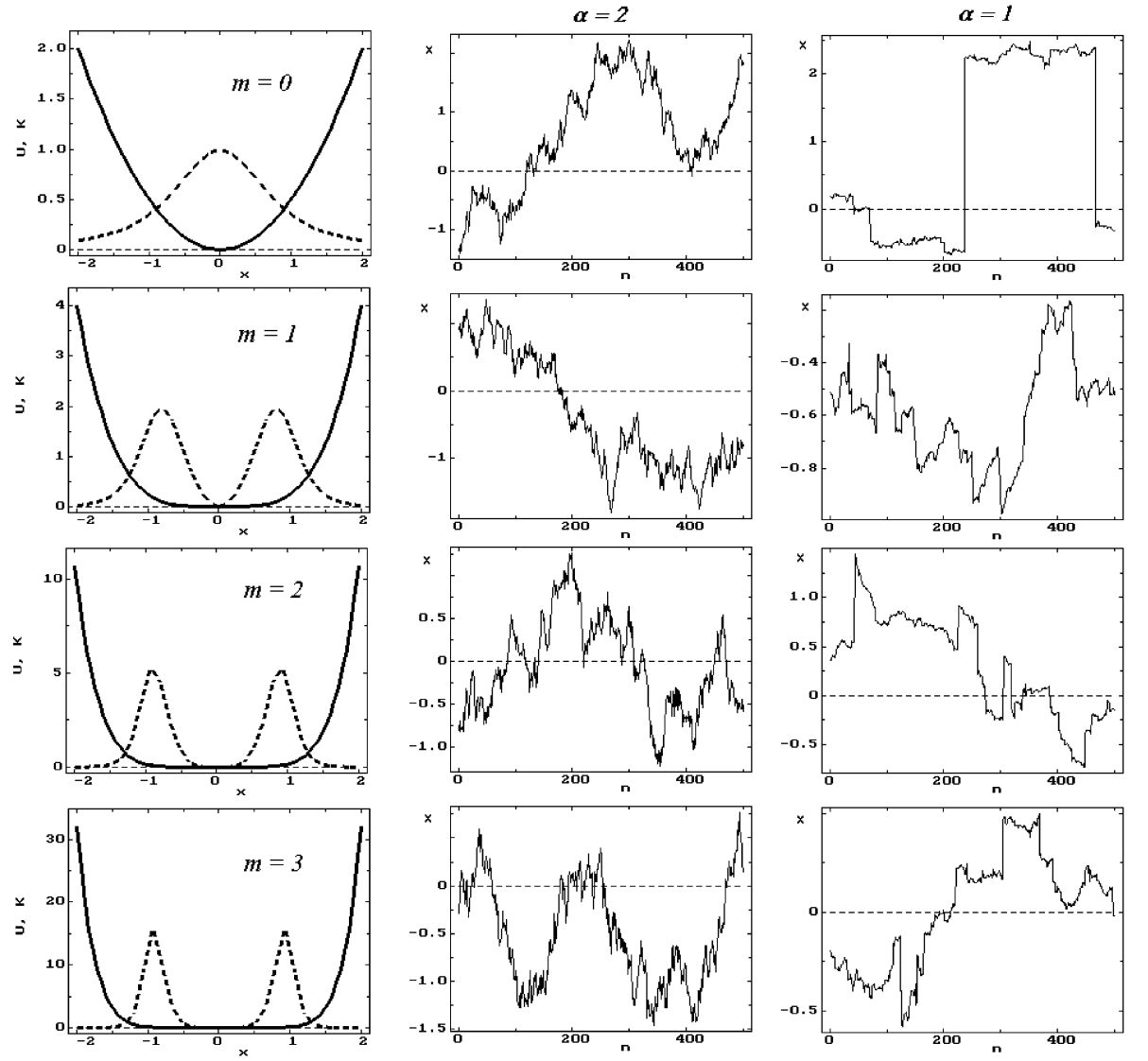

Fig. 7. Left column: the potential energy functions, see Eq. (5.1), $b = 1$ (solid lines) and their curvatures (dotted lines) for different types of oscillators, from the linear oscillators, $m = 0$ (at the top) to the strongly non-linear oscillator, $m = 3$ (at the bottom). Middle column: typical sample paths of the Brownian oscillators, $\alpha = 2$, with the potential energy functions shown on the left. Right column: typical sample paths of the Lévy oscillators, $\alpha = 1$.

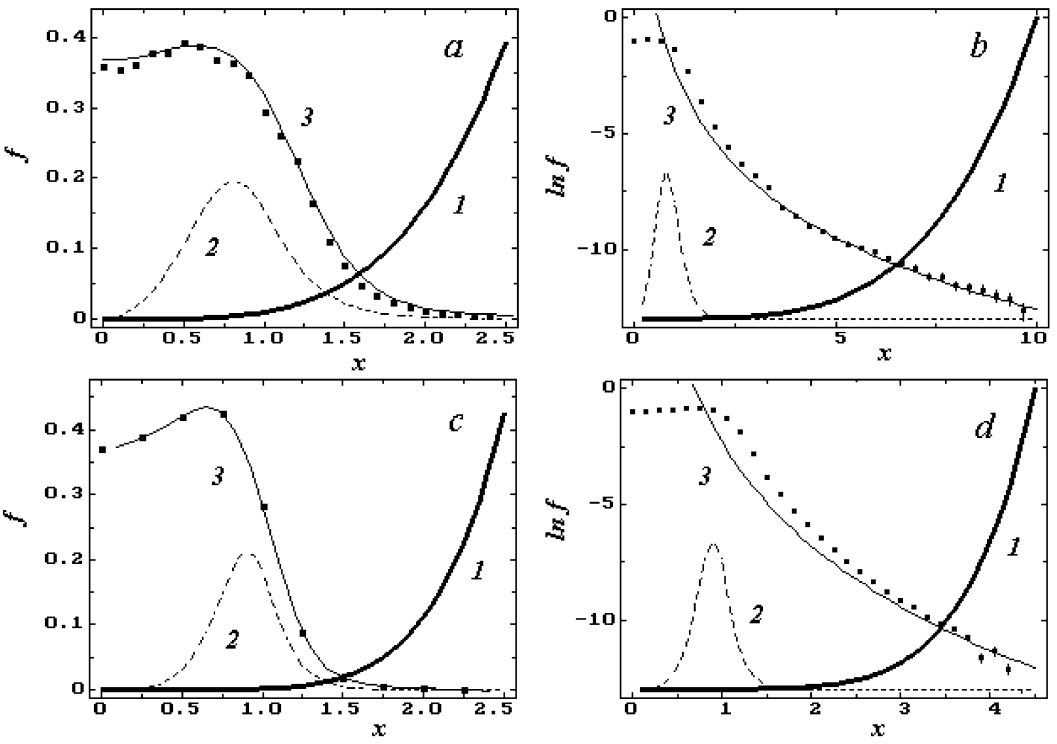

Fig. 8. Comparison of analytical calculations with the results of numerical modeling based on the solution of the Langevin equation. The order of the fractional derivative and the Lévy index of the white Lévy noise are equal to 1.5. At the top $m = 1$, at the bottom $m = 2$. For detailed explanation see Section 6.

Fig. 7 has an illustrative purpose. Here typical sample paths are shown for different potential energy functions in the Langevin equation, $\delta t = 7 \times 10^{-4}$. In the left column the potential energy functions with different m indices are shown by the solid lines. The dotted lines indicate their curvatures. In the middle and in the right columns the typical sample paths are shown for the oscillators driven by the Gaussian noise and the Lévy noise with $\alpha = 1$, respectively. Each row corresponds to the oscillator with the index m indicated in the left column. It is seen that the typical sample paths for all the Brownian oscillators are nearly the same, consisting of small increments of the coordinate during each time step δt. This is the consequence of the exponential shape of the stationary Boltzmann PDFs, which prohibits large increments. In contrast, Lévy flights with large increments of x are clearly distinct in the figures of the right column. These flights appear due to the power-law asymptotics of the stationary PDFs, which permit large values of the increments to occur. The longest flights are realized in case of the linear Lévy oscillator, $m = 0$, because the PDF of the linear oscillator has the fattest tails. As it follows from Eq. (5.13), with m increasing, the power-law asymptotics become steeper, therefore, the flights become shorter, that is, the long flights occur more rarely. This effect is clearly seen in the right column, when comparing, for example, sample paths for the linear oscillator (at the top) with strongly non-linear oscillator (at the bottom).

In Fig. 8 we compare the analytical and numerical results for $m = 1$ (at the top) and $m = 2$ (at the bottom). The black points indicate the PDFs obtained from numerical solution of the Langevin equations, $\alpha = 1.5$. In the left, Figs. 8(a) and (b), the results at small values of the argument are

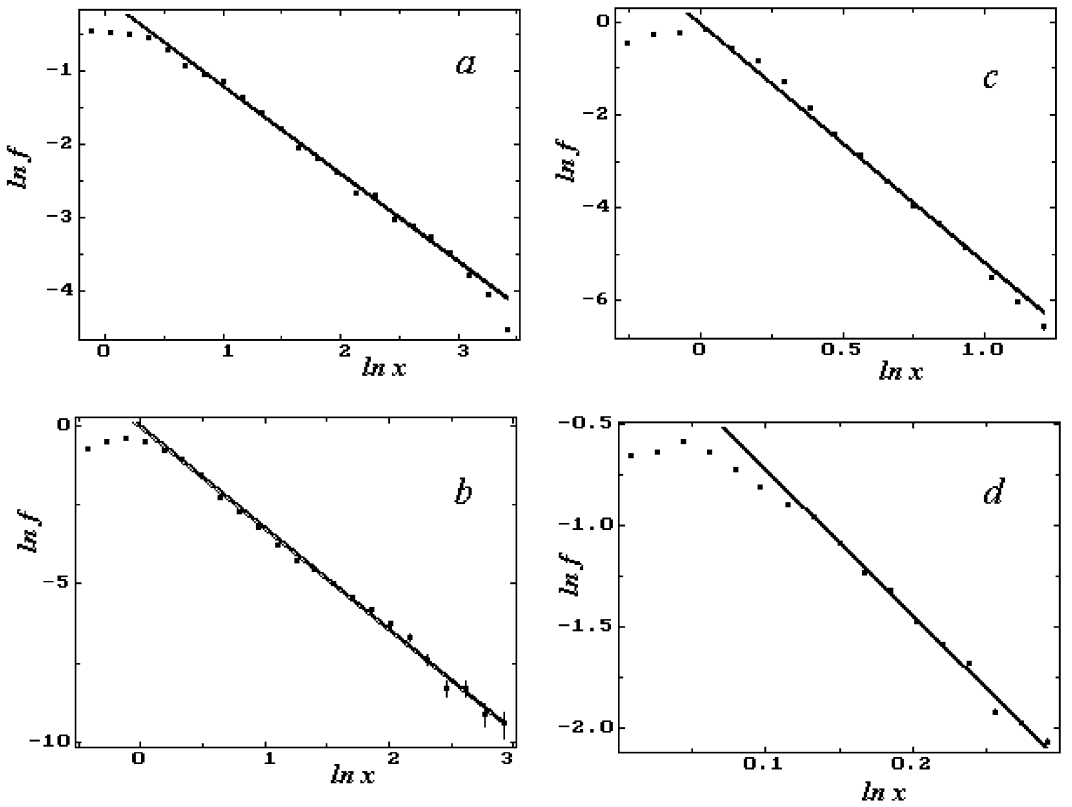

Fig. 9. Black points: stationary PDFs obtained by numerical solution of the Langevin equation for (a) $m = 0$, (b) $m = 1$, (c) $m = 2$, and (d) $m = 3$. The straight lines fit power-law asymptotics of the PDFs obtained by numerical simulation.

presented, where the bimodal character of the distributions is clearly seen. In the right, Figs. 8(c) and (d), the results are presented for large arguments, where the power-law asymptotics are clearly visualized. The potential energy functions $x^4/4$ (above) and $x^6/6$ (below) as well as their curvatures are shown by the solid lines 1 and dotted lines 2, respectively (in relative units on the vertical axis). In Fig. 8(a), the thin solid line indicates the PDF obtained by inverse Fourier transformation, using the continuation method, see Section 3. In Fig. 8(c) the black points are connected by a smooth solid curve. In Figs. 8(b) and (c) thin solid lines 3 show the asymptotics (5.13). It is seen that a good quantitative agreement exists between the results of the analytical estimates and the numerical simulation for stationary PDFs at small and large arguments, as well.

In Fig. 9 the PDFs obtained from the numerical modeling by statistical averaging are shown by black points in a log–log scale for: (a) $m = 0$, (b) $m = 1$, (c) $m = 2$, and (d) $m = 3$. The solid straight lines fit power-law asymptotics of the PDFs. In the numerical modeling the Lévy index is 1.2, $\delta t = 7 \times 10^{-4}$ for $m = 0$ and 1, and $\delta t = 10^{-4}$ for $m = 2$ and 3. For the statistical averaging 10^3 sample paths are used, each consisting of 5×10^3 time steps for $m = 0$ and 1, and 10^5 time steps for $m = 2$ and 3. The solid straight lines fit power-law asymptotics of the PDFs. The results of fitting are summarized in Fig. 10. Here γ is the power-law index in a log–log scale. In the numerical simulation it is defined as a tangent of a slope of the fitting line in Fig. 9. The values of γ are shown by black points for different α's and m's. The straight lines demonstrate the relation $\gamma = \alpha + 2m$, that is,

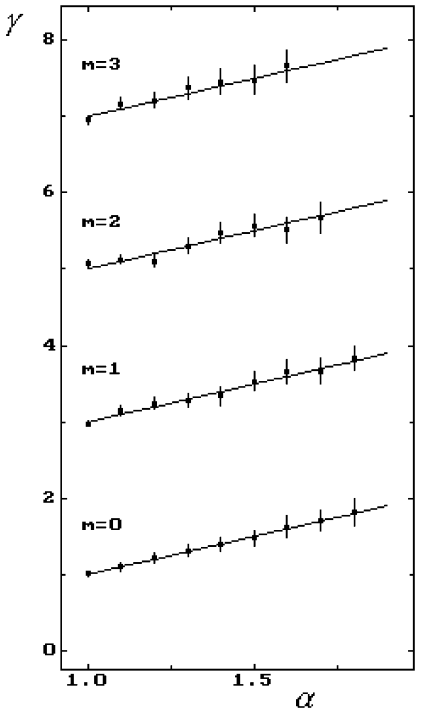

Fig. 10. The results of fitting the power-law asymptotics of the PDFs obtained by numerical simulation. Each black point indicates the tangent γ of the slope of the fitting line from Fig. 9 for the particular value of Lévy index α of the white noise. The straight lines demonstrate the relation $\gamma = \alpha + 2m$, see Eq. (5.13).

the analytical value of the power-law index in a log–log scale, see Eq. (5.13). A good quantitative agreement between analytical and numerical results is obvious.

7. Results

In this paper we study the properties of stationary states of overdamped non-linear Lévy oscillators driven by Lévy stable noise. The potential energy functions of the non-linear oscillators considered are $U(x) = bx^{2m+2}/(2m+2)$, where $m = 0$ (linear Lévy oscillator), $m = 1$ (quartic Lévy oscillator), $m = 2, 3, \ldots$ (strongly non-linear Lévy oscillators), and $U(x) = ax^2/2 + bx^4/4$, $a > 0$ (anharmonic Lévy oscillator). Our analytical approach is based on the solution of the fractional kinetic equation, which contains fractional space derivative of the order $\alpha, 1 \leqslant \alpha \leqslant 2$. Our numerical approach is based on the numerical solution of the Langevin equation with Lévy stable noise having Lévy index α which equals the order of the space derivative in the kinetic equation. The particular case $\alpha = 2$ corresponds to Brownian motion. In this case the kinetic equation has the well-known Boltzmann stationary solution, which is unimodal and decays exponentially at large $|x|$ values. The particular case $m = 0$ corresponds to the linear Lévy oscillator. In this case the fractional kinetic equation has a Lévy stable stationary solution, which is also unimodal and has long power-law asymptotics, therefore, the variance is infinite. We find that the properties of stationary probability for non-linear Lévy oscillators are radically different from the properties of the two cases mentioned above:

1. The stationary probability density functions have two humps. The bimodality is most pronounced for $\alpha = 1$. With α increasing, the effect becomes weaker, and it vanishes at $\alpha = 2$. On the other hand, for the anharmonic Lévy oscillator, Eq. (4.3), with the parameter a increasing, the bimodal shape also smoothes out, and at some critical value of a it turns into the unimodal one.

2. The stationary probability density functions have power-law asymptotics, which behave as $|x|^{-(\alpha+2m+1)}$ at $|x| \to \infty$. Thus, the variance is finite for non-linear Lévy oscillators, $m > 0$. For steeper potential energy functions the asymptotics decay more rapidly, and the Lévy flights become shorter.

The two features demonstrate the unusual statistical properties of systems driven by Lévy noises. They serve as the challenge for thermostatistics trying to explain non-Gibbsian phenomena. Applications of the theory presented to particular processes are of great interest, as well.

Acknowledgements

The authors thank G. Voitsenya for help in numerical simulation, and R. Gorenflo, F. Mainardi and I. M. Sokolov for fruitful discussions. This work is supported by the INTAS Project 00-0847. RM acknowledges financial support from

the Deutsche Forschungsgemeinschaft (DFG) within the Emmy Noether programme. AC acknowledges support from the DAAD.

References

[1] S. Chandrasekhar, Rev. Mod. Phys. 15 (1943) 1.
[2] N.G. Van Kampen, Stochastic Processes in Physics and Chemistry, North-Holland, Amsterdam, 1981.
[3] Yu.L. Klimontovich, Statistical Physics, Harwood, New York, 1986.
[4] B.D. Hughes, Random Walks and Random Environments, Volume 1: Random Walks, Oxford University Press, Oxford, 1995.
[5] H. Risken, The Fokker–Planck Equation, Springer, Berlin, 1996.
[6] R. Balescu, Statistical Dynamics, Matter Out of Equilibrium, Imperial College Press, London, 1997.
[7] P. Lévy, Theorie de l'addition des variables al'eatories, Gauthier-Villiars, Paris, 1937.
[8] B.V. Gnedenko, A.N. Kolmogorov, Limit Distributions for Sums of Independent Random Variables, GITTL, Moscow, 1949 (in Russian; Engl. Transl.: Addison-Wesley, Reading, MA, 1954).
[9] The wonderful world of stochastics: a tribute to E.W. Montroll, in: M.F. Shlesinger (Ed.), Studies in Statistical Mechanics, vol. 12, North-Holland, Amsterdam, 1985.
[10] J.-P. Bouchaud, A. Georges, Phys. Rep. 195 (1990) 127.
[11] J. Klafter, M.F. Shlesinger, G. Zumofen, Phys. Today 49 (2) (1996) 33.
[12] M.F. Shlesinger, G.M. Zaslavsky, J. Klafter, Nature 363 (1993) 31.
[13] R. Metzler, J. Klafter, Phys. Rep. 339 (2000) 1.
[14] A.Y. Khintchine, P. Lévy, C.R. Acad. Sci. Paris 202 (1936) 374.
[15] B.D. Hughes, Proc. Natl. Acad. Sci. USA 78 (1981) 3287.
[16] V. Seshadri, B.J. West, Proc. Natl. Acad. Sci. USA 79 (1982) 4501.
[17] M.F. Shlesinger, G.M. Zaslavsky, U. Frisch (Eds.), Lévy Flights and Related Topics, Springer, Berlin, 1995.
[18] P. Protter, D. Talay, Ann. Probab. 25 (1997) 393.
[19] J. Klafter, A. Blumen, M.F. Shlesinger, Phys. Rev. A 35 (1987) 3081.
[20] R. Metzler, E. Barkai, J. Klafter, Europhys. Lett. 46 (1999) 431.
[21] F. Mainardi, Y. Luchko, G. Pagnini, Fract. Calc. Appl. Anal. 4 (2001) 153.
[22] R. Gorenflo, F. Mainardi, in: A. Carpinteri, F. Mainardi (Eds.), Fractals and Fractional Calculus in Continuum Mechanics, Springer, Wien and New York, 1997, p. 223.
[23] B.J. West, V. Seshadri, Physica A 113 (1982) 203.
[24] F.E. Peseckis, Phys. Rev. A 36 (1987) 892.
[25] H.C. Fogedby, Phys. Rev. Lett. 73 (1994) 2517.
[26] J. Honkonen, Phys. Rev. E 53 (1996) 327.
[27] S. Jespersen, R. Metzler, H.C. Fogedby, Phys. Rev. E 59 (1999) 2736.
[28] A.V. Chechkin, V.Yu. Gonchar, J. Exp. Theor. Phys. 118 (2000) 730.
[29] Yu.L. Klimontovich, Statistical Physics in Open Systems, Kluwer Academic Publishers, Holland, 1994.
[30] D.D. Humieres, M.R. Beasly, B.A. Humberman, A. Libchaber, Phys. Rev. A 26 (1982) 3483.
[31] Yu.L. Bolotin, V.Yu. Gonchar, M.Ya. Granovsky, A.V. Chechkin, J. Exp. Theor. Phys. 88 (1999) 196.
[32] Yu.L. Bolotin, V.V. Bulavin, A.V. Chechkin, V.Yu. Gonchar, Prog. Nucl. Energy 35 (1999) 65.
[33] G. Samorodnitsky, M.S. Taqqu, Stable Non-Gaussian Random Processes, Chapman & Hall, New York, 1994.
[34] A.V. Skorokhod, Random Processes with Independent Increments, Nauka, Moscow, 1986 (in Russian; Engl. Transl.: Kluwer Academic Publishers, Dordrecht, 1991).
[35] A.I. Saichev, G.M. Zaslavsky, Chaos 7 (1997) 753.
[36] S.G. Samko, A.A. Kilbas, O.I. Marichev, Fractional Integrals and Derivatives, Theory and Applications, Nauka i Teknika, Minsk, 1987 (in Russian; Engl. transl.: Gordon and Breach, Amsterdam, 1993).
[37] I.M. Sokolov, J. Klafter, A. Blumen, Phys. Rev. E 64 (2001) 021107.
[38] G.H. Hardy, Divergent Series, Oxford, 1949.
[39] E. Kamke, Differentialgleichungen, Lösungsmethoden und Lösungen, Leipzig, 1959.
[40] A.V. Chechkin, V.Yu. Gonchar, Physica A 27 (2000) 312.